DOI: 10.26599/FSHW.2026.9251241

Contents lists available at SciOpen

Food Science and Human Wellness

journal homepage: https://www.sciopen.com/journal/2097-0765

China Food Publishing Co.

Alkaloids from *Zanthoxylum bungeanum* Maxim. alleviate MASLD *via* dual modulation of cannabinoid receptors and activation of Akt/GSK3β/Nrf2 signaling

Wenyi Liang[a,1], Heying Yang[a, b,1], Yaqian Duan[a], Chi Zhang[a], Songzhang Shen[a,*], Ting Han [a,*], Juan Su[a,b,*]

[a]*School of Pharmacy, Naval Medical University, Shanghai, 200433, China*

[b]*School of medicine, Shanghai University, Shanghai, 200444, China*

ABSTRACT: Metabolic dysfunction-associated steatotic liver disease (MASLD) represents a growing global health challenge, necessitating the discovery of safe and effective therapeutic agents from natural dietary sources. *Zanthoxylum bungeanum* Maxim. (*huajiao*), a widely consumed pharma-food, contains abundant alkaloids with reported lipid-regulating, antioxidant, and anti-inflammatory activities, but its underlying mechanisms against MASLD remain unclear. This study aimed to evaluate the hepatoprotective effects of alkaloids from *Z. bungeanum* (ZBA) and elucidate its molecular targets using an integrated approach combining network pharmacology, transcriptomics, and experimental validation. To this end, FFAs-stimulated HepG2 cells and HFD-fed mice were employed to assess the effects of ZBA. The results showed that ZBA significantly alleviated hepatic lipid accumulation, improved insulin sensitivity, and reduced systemic inflammation. Mechanistically, omics analysis and molecular docking predicted the endocannabinoid system as a key target, and the cellular thermal shift assay confirmed that ZBA directly binds to both CB1 and CB2 receptors. Furthermore, pharmacological interventions using specific agonists and antagonists revealed that ZBA exerts a dual modulatory effect on the endocannabinoid system by suppressing CB1 overexpression and enhancing CB2 activity. This modulation subsequently activates the Akt/GSK3β/Nrf2 signaling cascade to restore lipid metabolism homeostasis and mitigate lipotoxicity in a dose-responsive regulatory trend. In conclusion, the present findings highlight that ZBA ameliorates MASLD by rebalancing the expression of CB1 and CB2 receptors, thereby modulating Akt/GSK3β/Nrf2 axis, thus providing a scientific basis for the development of ZBA as a functional food ingredient for metabolic health.

Keywords: *Zanthoxylum bungeanum* Maxim., cannabinoid receptor, alkaloid, metabolic dysfunction-associated steatotic liver disease

1. Introduction

Metabolic dysfunction-associated steatotic liver disease (MASLD) represents a complex hepatic metabolic condition arising from the interplay of multiple pathological factors, such as aberrant lipid metabolism, insulin resistance, and sustained inflammatory responses [1]. It manifests as a pathological

[1]These authors contributed equally to this work.
***Corresponding author**
Juan Su, juansu_2008@126.com; Ting Han, than927@163.com;
Songzhang Shen, 13817781446@126.com

Received 8 December 2025
Received in revised from 8 February 2026
Accepted 16 July 2026

continuum, initiating as simple hepatic steatosis and potentially advancing through metabolic dysfunction-associated steatohepatitis to more severe stages including fibrosis, cirrhosis, and ultimately hepatocellular carcinoma. MASLD currently stands as the predominant chronic liver disorder worldwide affecting over 30% of the global adult population [2]. Despite its increasing prevalence, effective pharmacological interventions for MASLD remain limited, and conventional single-target therapeutic strategies often exhibit unsatisfactory efficacy [3, 4].

In recent years, increasing attention has been directed toward natural food-derived bioactive compounds and medicine-food homology materials for MASLD management [5, 6]. Owing to their multi-component and multi-target characteristics, these natural products are capable of simultaneously regulating lipid metabolism, oxidative stress, inflammation, and insulin sensitivity, thereby demonstrating unique advantages in the dietary intervention of metabolic diseases [7, 8]. Moreover, many edible natural materials possess favorable long-term safety profiles and thus hold considerable potential for functional food development. Previous studies have shown that food-derived active compounds such as ginsenosides and plant polyphenols can ameliorate hepatic steatosis and inflammatory responses through coordinated modulation of multiple metabolic pathways [9, 10]. The continuous exploration of effective dietary active ingredients and their molecular mechanisms may provide important scientific evidence for the development of nutritional strategies targeting liver health.

Accumulating evidence has demonstrated that the endocannabinoid system plays a crucial role in the pathogenesis and progression of MASLD. The endocannabinoid system consists of endogenous cannabinoids, metabolic enzymes, and the classical cannabinoid receptors CB1 and CB2, which are critically involved in regulating hepatic lipid metabolism, glucose homeostasis, inflammation, and fibrogenesis [11-13]. Under pathological metabolic conditions, hepatic CB1 expression is significantly upregulated and contributes to de novo lipogenesis, insulin resistance, and hepatic steatosis through suppression of insulin signaling and promotion of lipid accumulation [14]. In contrast, CB2 mainly exerts anti-inflammatory and anti-fibrotic effects by inhibiting macrophage activation and inflammatory cytokine production [15, 16]. Therefore, dual modulation of CB1 and CB2 has emerged as a promising therapeutic strategy for MASLD and related metabolic disorders [17]. However, natural food-derived compounds capable of simultaneously regulating both cannabinoid receptors remain insufficiently explored.

Huajiao, as a traditional Chinese medicinal and edible spice, refers to the dried pericarps of plants from two subgenera of the genus *Zanthoxylum* in the Rutaceae family, namely *Zanthoxylum bungeanum* Maxim. (*Z. bungeanum*) and *Zanthoxylum schinifolium* Sieb. et Zucc. [18]. In addition to its characteristic pungent flavor, *huajiao* contains abundant bioactive constituents including alkaloids, flavonoids, volatile oils, coumarins, and terpenoids [19, 20]. Among these, alkaloids have attracted extensive attention because of their prominent lipid-lowering, antioxidant, and anti-inflammatory activities [21-23]. Previous studies demonstrated that alkaloids from *Z. bungeanum* (ZBA) could improve glucose and lipid metabolism by enhancing GLUT2 expression, suppressing SREBP-1c-mediated lipogenesis, and promoting fatty acid β-oxidation through

activation of the PPARα pathway [24, 25]. Hydroxy-α-sanshool, one of the major alkaloids in *huajiao*, was also reported to regulate energy metabolism and adipose browning through activation of TRPV1 and downstream metabolic signaling pathways [26]. Nevertheless, the amelioration of ZBA in MASLD remain insufficiently understood, particularly regarding their potential regulatory role in the endocannabinoid system. Therefore, the present study comprehensively investigated the effects of ZBA on MASLD and elucidated its molecular mechanisms *via* integrated network pharmacology, transcriptomic, molecular docking, and experimental validation, aiming to provide a solid scientific foundation for its subsequent application in functional foods or dietary intervention for liver health.

2. Methods

2.1 The preparation of the alkaloids from Z. bungeanum (ZBA)

The ZBA was obtained using a previously optimized method [27]. In short, the pericarps were obtained from *Z. bungeanum* (commonly known as 'hong *huajiao*' or Sichuan pepper) produced in Hanyuan, Sichuan, China (Batch No. 23092105). 100 g of Z. *bungeanum* pericarps underwent reflux extraction with 1000 mL of 50% aqueous ethanol at 95°C for 1 h, a process repeated third. The combined filtrates were concentrated to 500 mL and then loaded onto a Mitsubishi HP-20 macroporous resin column to remove impurities. The eluate was concentrated in vacuo at 45°C and then lyophilized to yield the final ZBA powder. The chemical characterization of ZBA was qualitatively and quantitatively analyzed. A total of 22 alkaloid compounds were identified in ZBA, including 20 amide alkaloids, one quinoline alkaloid, and one isoquinoline alkaloid. Among these, the contents of hydroxy-α-sanshool and hydroxy-β-sanshool were 4.71% and 1.02%, respectively.

2.2 Cell culture and CCK-8 assay

HepG2 cells, sourced from the Stem Cell Bank of the Chinese Academy of Sciences, were cultured in complete MEM medium supplemented with 10% FBS and 1% penicillin-streptomycin at 37°C with 5% CO_2. For the cell viability assay, cells were seeded into 96-well plates (1×10^5 cells/well) overnight and then treated with serial doses of ZBA (25-200 μg/mL) or simvastatin (2-32 μM) for 24 h. Subsequently, the medium was replaced with fresh MEM containing 10% CCK-8 reagent and incubated for 1.5 h. The optical density at 450 nm was determined with Shanpu microplate reader.

2.3 Cell treatment

Based on the experimental results of cell viability, appropriate drug concentrations were selected for *in vitro* pharmacological evaluation. HepG2 cells in the logarithmic growth phase were harvested and prepared into a cell suspension. The cells were seeded into 6-well plates (2×10^5 cells/well) and incubated for 24 h. After incubation, the original culture medium was removed, and the cells were gently washed with PBS buffer. Subsequently, the cells were subjected to different treatments as follows: the normal group received 2 mL of complete medium; the model group was treated with 2 mL of complete medium containing 0.3 mM free fatty acids (FFAs); the ZBA-treated groups and the positive group were exposed to complete medium

containing 0.3 mM FFAs along with corresponding drugs. In the ZBA-treated groups, concentrations of 50 and 75 μg/mL ZBA were applied, while the PC group received 4 μM simvastatin. After 24 h of intervention, the culture was terminated and subsequent assays were performed.

To elucidate the upstream regulatory role of CB1/CB2 in the Akt/GSK3β/Nrf2 signaling pathway, a pharmacological intervention experiment was performed using specific agonists and antagonists. HepG2 cells were seeded into 6-well plates and cultured overnight. The cells were then randomly divided into four groups: control group (treated with vehicle), model group (stimulated with 0.3 mM FFAs), CB1 inhibition group (co-treated with 0.3 mM FFAs and 1 μM Rimonabant, a CB1 antagonist), and CB2 activation group (co-treated with 0.3 mM FFAs and 1 μM JWH-133, a CB2 agonist). Following the 24-hour incubation, cells were harvested, and the expression levels of key proteins in the Akt/GSK3β/Nrf2 pathway were analyzed by Western blotting.

2.4 Animal experiments

All *in vivo* experiments were conducted under a protocol approved by the Animal Experimental Research Center of Naval Medical University (Approval No. 2023107). normal standard diet (PD405J) and high fat diet (PD6001) was obtained from the SYSE BIO Institute Co. Seven-week-old male C57BL/6J mice, sourced from Hangzhou Ziyuan Animal Technology Co., Ltd., were housed under controlled conditions (12 h light/dark cycle, 23 ± 2 °C, 47 ± 8% humidity) with *ad libitum* access to food and water. Following acclimation, the mice were allocated randomly into five groups (n = 8): normal group (normal diet, Normal), model group (high-fat diet, Model), positive group control (simvastatin, 8 mg/kg, PC), ZBA low-dose group (80 mg/kg, ZBA-L), and ZBA high-dose group (160 mg/kg, ZBA-H). With the exception of the normal group, all mice were fed a high-fat diet. Throughout the 12-week intervention, treatments were administered *via* oral gavage once per day. After the final dose, animals were fasted overnight with water and then euthanized prior to collection of blood and liver tissues. Serum was subsequently separated from the blood by centrifugation at 3000 rpm for 15 min.

2.5 Oil Red O staining

To quantify intracellular lipid droplet formation, HepG2 cells were analyzed using Oil red O staining. Briefly, the culture medium was aspirated, and cells were washed three times with PBS. Upon complete removal of PBS, the cells were fixed with 4% paraformaldehyde for 20 min. After fixation, the cells were exposed to a freshly prepared Oil red O working solution for 15 min in the dark. Image acquisition were performed by an Olympus microscope. For quantification, intracellular lipids were dissolved in 300 μL isopropanol per well under dark shaking for 30 min, and then the absorbance of dissolved dye was measured at 518 nm. To clarify the lipid accumulation in the liver tissues, we froze, embedded, and sectioned them into 10 μm slices. The staining protocol involved a 15-min fixation step using 4% polyformaldehyde, followed by a 10-min incubation with Oil red O solution. Subsequently, the slides were coverslipped with glycerin gelatin, and lipid droplet deposition was examined under an Olympus microscope.

2.6 Biochemical and cytokine analysis

Assay kits for biochemical analyses were acquired from the Nanjing Jiancheng Institution, including those for total cholesterol (TC), triglyceride (TG), non-esterified fatty acids (NEFA), low density lipoprotein cholesterol (LDL-C), high-density lipoprotein cholesterol (HDL-C), aspartate aminotransferase (AST), and alanine aminotransferase (ALT). The cellular cytokines (IL-1β, IL-6, and TNF-α) were determined by ELISA kits (UpingBio, Hangzhou, Chian). All operations are performed according to the manufacturers' instructions.

2.7 Glucose tolerance test (GTT) and insulin tolerance test (ITT)

For GTT, mice were fasted for 12 h with free access to water. After baseline blood glucose measurement at 0 min, glucose solution (2 g/kg, 20% w/v) was administered by intragastric gavage. Tail vein blood samples were collected at 15, 30, 60 and 120 min post-administration for blood glucose measurement using using a glucometer (Roche, Switzerland). For ITT, mice were subjected to a 4 h fast before intraperitoneal injection of insulin (1 U/kg, Wanbang, China). Blood glucose levels were monitored at 15, 30, 60 and 120 min. Area under the curve (AUC) for blood glucose was calculated.

2.8 Hematoxylin-eosin (H&E) staining

To evaluate liver pathology, mouse liver tissues were processed for H&E staining. Briefly, tissue samples were fixed in 4% polyformaldehyde and subsequently dehydrated through a graded ethanol series prior to paraffin embedding. Sections were cut at a thickness of 5 μm and stained with hematoxylin and eosin for microscopic evaluation.

2.9 Transcriptome sequencing

Liver tissues from the normal, model, and ZBA-H groups were subjected to transcriptome sequencing. Total RNA was extracted and its quality was assessed by measuring purity and concentration, evaluating integrity, and determining the RQN value. Qualified RNA libraries were constructed and clustered on a cBot system, followed by sequencing on the Illumina NovaSeq platform for 150 bp paired-end reads. Subsequently, the DESeq2 package (v1.26.0) was applied to identify differentially expressed genes, and their functional implications were explored *via* Gene Ontology (GO) and the Kyoto Encyclopedia of Genes and Genomes (KEGG) enrichment analyses implemented in Python package.

2.10 Network pharmacology analysis

The putative targets of 22 components identified from ZBA were systematically investigated using TCMSP database (https://old.tcmsp-e.com/tcmsp.php), SwissTargetPrediction (http://swisstargetprediction.ch/) and TargetNet database (http://targetnet.scbdd.com/). Meanwhile, disease-associated targets for MASLD were retrieved from the OMIM (https://omim.org/), GeneCards (https://www.genecards.org/cgi-bin/carddisp.pl), and DrugBank (https://www.drugbank.com/) database. The overlapping portion of the two target sets was considered a potential target for ZBA in treating MASLD. Protein–protein interaction (PPI), filtered with a confidence score threshold of 0.4, was obtained from the STRING database (https://string-db.org). The compound-target network was built by Cytoscape 3.9.1

software. To elucidate the biological functions and pathways involved, GO and KEGG enrichment analyses were performed.

2.11 Molecular docking

The two-dimensional structures of the compounds were acquired from the PubChem database, and their three-dimensional conformations were generated using ChemBio3D Ultra 15.0. The crystal structures of the candidate target proteins were retrieved from the RCSB Protein Data Bank (https://www.rcsb.org/), with the following PDB IDs: CB1 (5U09), Akt (3O96), GSK3β (1SGO), TLR4 (3FXI), MTOR (1FAP), MMP9 (1GKC), and APP (8JAL). All protein structures underwent pre-docking preparation, which included the removal of water molecules and native ligands, followed by the addition of hydrogen atoms. Molecular docking simulations were then conducted with AutoDock Vina 1.1.2 to calculate binding affinities, and the resulting docking poses were visualized with PyMOL 3.1.3. A binding energy threshold of ≤ -5.0 kcal/mol was set as the criterion for a favorable interaction, with more negative values indicating higher binding stability.

2.12 Cellular thermal shift assay (CETSA)

HepG2 cells were seeded and cultured in 0.3 mM FFAs for 24 h. After that, cells were harvested and then aliquoted into six equivalent samples. These samples were co-treated with 75 μg/mL ZBA for a duration of 2 h. Subsequently, the cell suspensions underwent a thermal denaturation protocol, being heated at different temperatures ranging from 37°C to 52°C with a step of 3°C for 3 min. Protease inhibitor was added and cells were lysed by repeated freeze-thaw in liquid nitrogen. The supernatants were prepared by centrifugation at 14,800 rpm for 10 min at 4°C.

2.13 Immunohistochemistry

Following fixation with 4% paraformaldehyde, liver tissues were embedded in paraffin and sliced into 4-μm sections. The sections were then dewaxed in xylene, rehydrated through a graded alcohol series, and subjected to microwave-heating-mediated antigen retrieval. Endogenous peroxidase activity was quenched, followed by blocking with 3% BSA for 30 min at room temperature. The sections were subsequently incubated separately with anti-TNF-α, anti-IL-1β, and anti-IL-6 antibodies at 4°C overnight. The secondary antibody was added and reacted for 50 min. DAB and hematoxylin were used for staining. The processed slides were finally sealed, digitally scanned, and analyzed. Antibodies for IL-1β were procured from Abcam. Antibodies for IL-6, and TNF-α were obtained from Invitrogen.

2.14 Western blotting

Protein lysates were prepared from mouse liver tissues or cultured HepG2 cells and quantified prior to immunoblotting. Separation was achieved on 10% SDS-polyacrylamide gels, followed by electroblotting onto PVDF membranes with a pore size of 0.45 μm. Membranes were blocked for 1 h before an overnight incubation at 4°C with specifically diluted primary antibodies. Following extensive washes with TBST, the membranes were incubated with an appropriate horseradish peroxidase (HRP)-conjugated secondary

antibody for 2 h. The target proteins were detected by chemiluminescence and photographed. Antibodies against CB1, Akt, p-Akt Ser473, GSK3β, p-GSK3β Ser9, and Nrf2 were obtained from Cell Signaling Technology. Antibodies for p-Nrf2 Ser40 and CB2 were procured from Abcam and Invitrogen, respectively.

2.15 Statistics

All quantitative data were presented as mean ± standard deviation, and then they were processed and graphically visualized utilizing GraphPad Prism 7. For comparisons across multiple experimental groups, one-way analysis of variance (ANOVA) was applied, followed by post *hoc* Tukey for detailed group-wise comparisons. A *p*-value of less than 0.05 was considered statistically significant.

3. Results

3.1 ZBA ameliorated lipid dysregulation in FFAs-stimulated HepG2 cells

An *in vitro* model of hepatic steatosis was established by treating HepG2 cells with FFAs for 24 h to assess the lipid-lowering potential of ZBA. CCK-8 assay defined the non-toxic concentration range of ZBA, observing that ZBA at 75 μg/mL maintained cell viability at 90.4% (Fig. 1A), leading to the selection of 50 and 75 μg/mL for subsequent experiments. Similarly, the concentrations for simvastatin and FFAs were set at 4 μM and 0.3 mM, respectively (Fig. 1B-C). Oil red O staining revealed that abundant densely distributed red lipid droplets in the cytoplasm of the FFAs-induced model group (Fig. 1D-E), which was corroborated by a significant increase in absorbance of dissolved stain compared to normal cells (Fig. 1F). ZBA treatment, particularly at 75 μg/mL (ZBA-H), markedly reduced lipid droplet number and size, and decreased absorbance by approximately 60% relative to the model group (Fig. 1F). Furthermore, the FFAs-induced elevations in intracellular TC and TG levels were also significantly reversed by ZBA co-treatment (Fig. 1G-H). These findings collectively evidence the efficacy of ZBA in ameliorating lipid metabolic dysregulation *in vitro*.

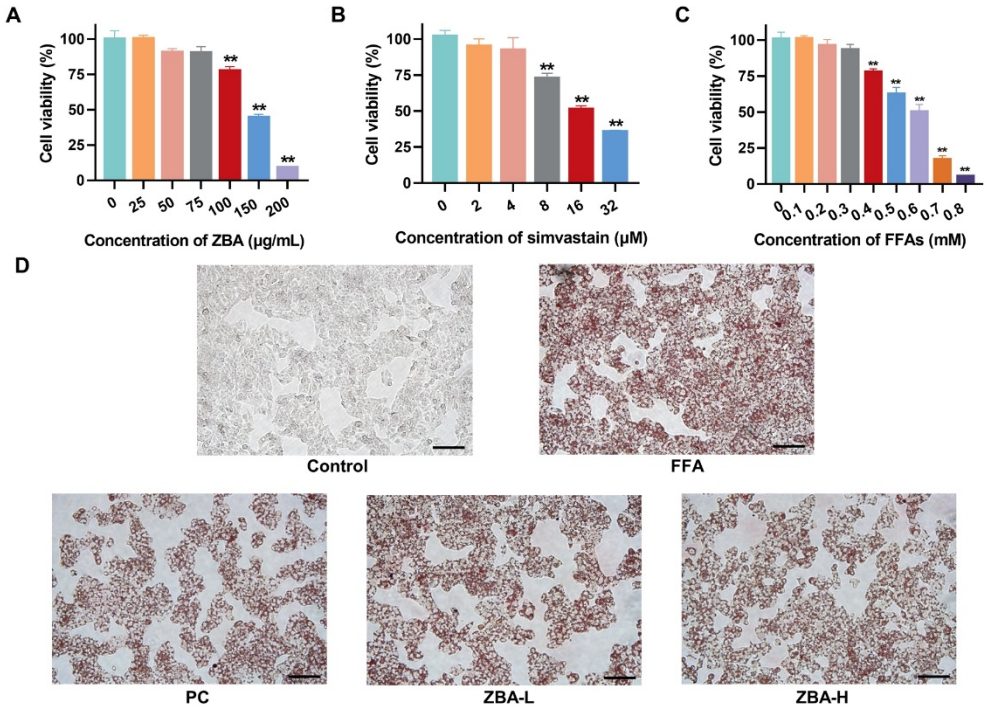

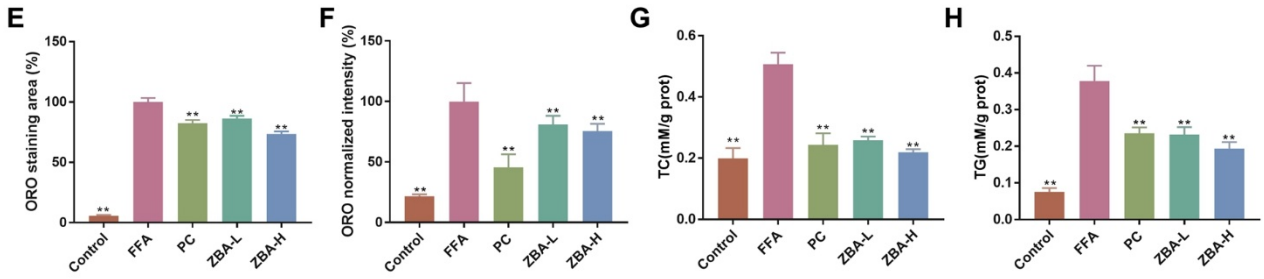

Fig. 1 Effects of ZBA on lipid accumulation in FFAs-induced HepG2 cells. Normal, vehicle; Model, 0.3 mM FFAs; PC, 0.3 mM FFAs + 4 μM simvastatin; ZBA-L, 0.3 mM FFAs + 50 μg/mL ZBA; ZBA-H, 0.3 mM FFAs + 75 μg/mL ZBA. (A-C) The vitality of cells against ZBA, simvastatin and FFAs. (D-F) Representative images and quantitative results for oil red O staining of HepG2 cells (200×, scale bar = 100 μm). (G-H) Intracellular TC and TG levels. *$P < 0.05$, **$P < 0.01$, compared with the model group.

3.2 ZBA ameliorated MASLD phenotype in HFD-fed mice

The benefits of ZBA was further investigated in a murine MASLD model induced by a 12-week HFD regimen. Initial body weights were comparable across all groups. However, ZBA administration (80 and 160 mg/kg) exerted a dose-dependent suppression on HFD-promoted weight gain (Fig. 2A). Notably, the body weight reduction induced by ZBA was not attributed to alterations in food intake, as no inhibitory effects on appetite or feeding behavior were detected (Fig. 2B). The macroscopic observation showed that livers from the model group exhibited steatotic features including enlarged volume, darkened coloration, visible yellowish lipid spots on the rough and dull surface, and significantly blunted margins. While ZBA treatment effectively reversed hepatic pathological alterations, reducing organ enlargement, restoring smoothness and elasticity of the surface, sharpening the margins, and diminishing visible spots (Fig. 3C). Consistent with this, histological and biochemical analyses confirmed the anti-steatotic effects of ZBA. While HFD feeding induced severe hepatic steatosis and vacuolation alongside extensive lipid droplet accumulation as observed by Oil red O staining, and ZBA intervention substantially alleviated these abnormalities (Fig. 3C). ZBA counteracted the HFD-induced elevations in hepatic TC and TG content (Fig. 3D-E). Serum profiling further demonstrated that ZBA favorably modulated lipid parameters, evidenced by reduced levels of TC, TG, NEFA, and LDL-C, coupled with an increase in HDL-C (Fig. S1). Moreover, ZBA treatment significantly reduced serum AST and ALT levels, indicating protection against lipid accumulation-induced hepatic injury (Fig. 3F-G). GTT and ITT further revealed that HFD feeding significantly impaired glucose tolerance and insulin sensitivity, whereas ZBA treatment dose dependently ameliorated these abnormalities (Fig. 3H-K). These findings underscore the protective role of ZBA in MASLD by rectifying both lipid and glucose metabolic disturbances as well as mitigating liver injury.

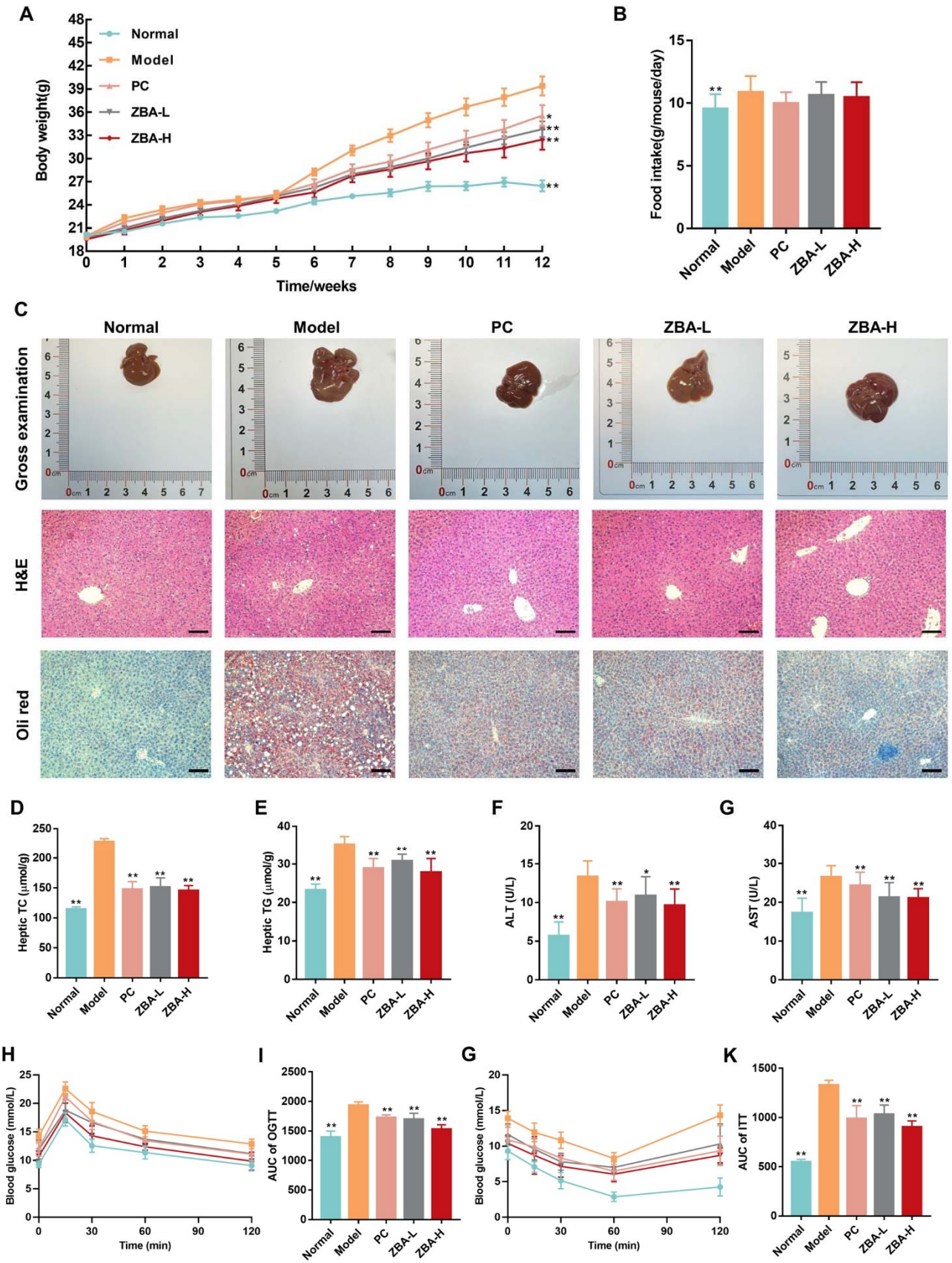

Fig. 2 Effects of ZBA on HFD-induced MASLD mice. Normal, normal diet; Model, HFD; PC, HFD + 8 mg/kg simvastatin; ZBA-L, HFD + 80 mg/kg ZBA; ZBA-H, HFD + 160 mg/kg ZBA. (A) Body weight monitored over the 12-week experimental period. (B) Average food intake of mice. (C) Representative images displaying liver gross morphology, H&E-stained sections, and Oil Red O-stained sections (200×, scale bar = 100 μm). (D-E) The hepatic levels of TC and TG. (F-G) The serum levels of ALT, and AST. (H-I) GTT, and the calculation of the corresponding area under the curve (AUC). (J-K) ITT, and the calculation of the corresponding AUC. *P < 0.05, **P < 0.01, compared with the model group.

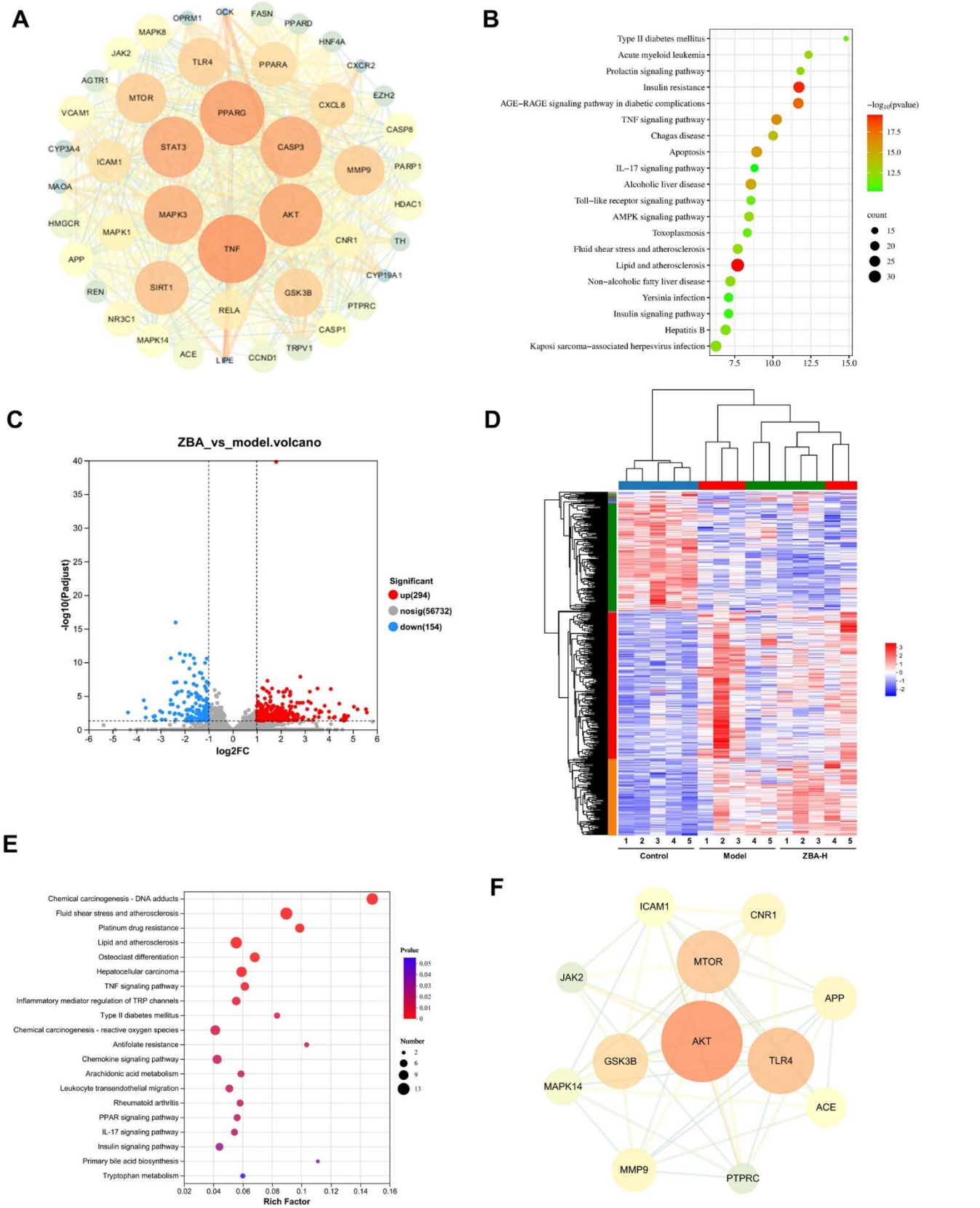

Fig. 3 Network pharmacology and transcriptomic analysis of ZBA treatment for MASLD. (A) The PPI network of ZBA-MASLD targets. (B) Functional enrichment analysis (top 20 KEGG pathways) of the overlapping targets identified through network pharmacology analysis. (C-D) Volcano plot and heatmap visualization of differentially expressed genes in liver tissues comparing model and ZBA-treated groups. (E) Functional enrichment analysis (top 20 KEGG pathways) of the differentially expressed genes identified through transcriptomic sequencing. (F) The core target PPI network constructed by integrating screening results from both network pharmacology and transcriptomic approaches.

3.3 The potential mechanism of ZBA on MASLD based on network pharmacology and transcriptomic

In order to systematically elucidate the mechanism by which ZBA improves MASLD, we explored the potential and multiple interactions between ZBA and MASLD by network pharmacology and transcriptomics. A total of 378 candidate targets associated with ZBA were identified through SwissTargetPrediction and TCMSP. A comprehensive collection of 2316 MASLD-associated targets was assembled from public repositories including GeneCards, OMIM, DisGeNET, and DrugBank. Intersection analysis of these datasets identified 195 overlapping targets, which were hypothesized to mediate the therapeutic effects of ZBA. Based on STRING-derived interactions, a compound-target network was constructed in Cytoscape 3.9.1, highlighted hydroxy-α-sanshool, hydroxy-β-sanshool, isobungeanool, qinbunamide A, and qinbunamide B as the top-ranked components in terms of connectivity, suggesting their roles as primary bioactive constituents (Table S1). Furthermore, 46 core targets were screened such as TNF, Akt, GSK3β, PPARG, MAPK (Fig. 3A). KEGG enrichment analysis identified prominent enrichment in pathways governing lipid and atherosclerosis, insulin signaling, and TNF signaling pathway (Figure 3B), suggesting these metabolic and inflammatory cascades constitute the core mechanistic underpinnings accounting for the therapeutic effects of ZBA.

Transcriptomic profiling of liver tissues revealed distinct gene expression patterns between the HFD model and ZBA-treated groups. Analysis of the volcano plot and heatmap identified 448 genetic variations following ZBA intervention, comprising 294 up-regulated and 154 down-regulated genes (Fig. 3C). The heatmap further demonstrated that ZBA treatment substantially reversed the dysregulated expression patterns induced by HFD (Fig. 3D). KEGG enrichment analysis of these differential genes indicates that the core biological processes primarily involved in ZBA include lipid metabolism, inflammation, and insulin resistance (Figure 3E). Consistent with network pharmacology predictions, modulation of inflammatory homeostasis alongside improved lipid metabolism and insulin signal transduction collectively forms the core network through which ZBA alleviates MASLD. By combining transcriptomic differentially expressed genes and network pharmacology-derived core targets, a PPI network was constructed to systematically explore the anti-MASLD mechanisms of ZBA. Seven overlapping core targets were screened based on node Degree values, including Akt, TLR4, mTOR, GSK3β, CNR1 (CB1), MMP9, and APP (Fig. 3F).

3.4 CB1 and CB2 were core targets for ZBA to attenuate MASLD

Molecular docking studies were performed to interrogate the interactions between core components and candidate targets. The computed binding energies and visualized docking poses revealed that CB1, Akt, and GSK3β all formed stable complexes with multiple alkaloids, exhibiting binding energies below the -5.0 kcal/mol threshold (Fig. 4A-F, Fig. S3 and Table S2). It suggested that the three potential targets might be crucial for the treatment of MASLD with ZBA. Hydroxy-α-sanshool bind to the pocket domain of CB1, forming three hydrogen bonds with the Ser85, His81 and Gln116 residue. Similarly, hydroxy-β-sanshool displayed a high binding affinity for CB1 (-6.9 kcal/mol). Given that their high content of ZBA, it was indicated that CB1 was the pivotal target for ZBA in ameliorating MASLD. CB1 and CB2 both belong to

the cannabinoid receptor family and exhibit high homology, thus CETSA was employed to analyze whether ZBA binds directly to CB1 or CB2. In vehicle-treated cells, the levels of CB1 and CB2 exhibited a temperature-dependent decline, becoming largely undetectable at 46°C and 49°C, respectively. In contrast, ZBA treatment significantly enhanced the thermal stability of both receptors, with detectable signals persisting up to 52°C (Fig. 4G-H). These findings suggest that ZBA forms stable interactions with both CB1 and CB2.

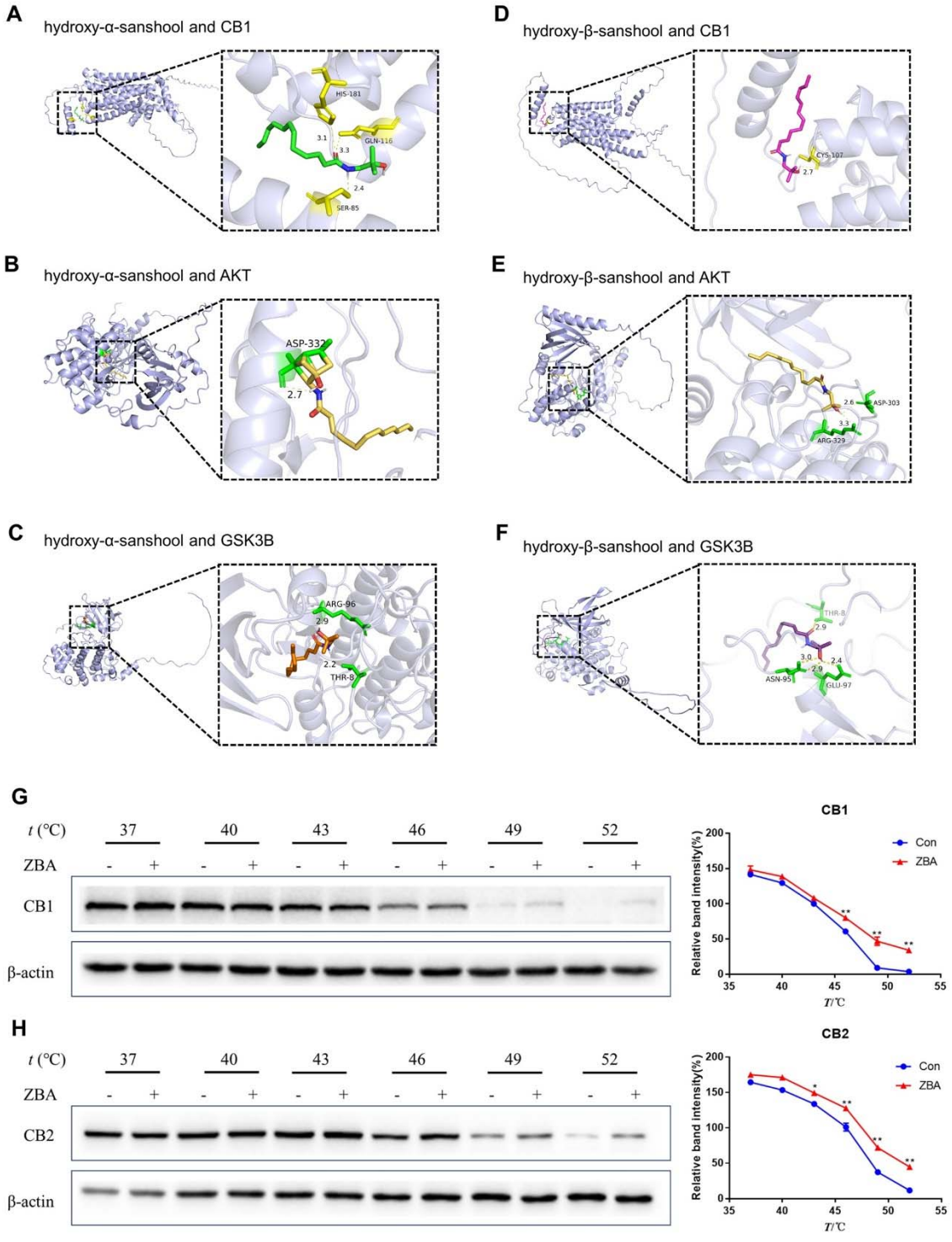

Fig. 4 The interaction between ZBA and potential core targets screened by network pharmacology and transcriptomics. (A-F) Molecular docking of the core active components of ZBA and potential targets (CB1, Akt and GSK3β). (G-H) CETSA assays of ZBA binding to CB1 and CB2.

3.5 CB1 and CB2 functionally regulate the Akt/GSK3β/Nrf2 pathway

Previous studies have demonstrated that the endocannabinoid receptors CB1 and CB2 are critically involved in MASLD pathogenesis [28-30]. Since transcriptomic and network pharmacology analyses identified Akt signaling potentially associated with CB1/CB2 regulation, pharmacological intervention experiments were further performed to clarify the functional relationship between cannabinoid receptors and Akt/GSK3β/Nrf2 signaling. As shown in Fig. 5A-C, FFAs stimulation significantly increased CB1 expression while decreasing CB2 expression in HepG2 cells compared with the control group. Treatment with the CB1 antagonist Rimonabant markedly suppressed CB1 expression, whereas the CB2 agonist JWH-133 significantly enhanced CB2 expression. Importantly, both Rimonabant and JWH-133 significantly restored Akt phosphorylation suppressed by FFAs, indicating that inhibition of CB1 or activation of CB2 could reactivate Akt signaling under steatotic conditions (Fig. 5D). Consistent with Akt activation, the phosphorylation levels of GSK3β and Nrf2 were also markedly increased following Rimonabant or JWH-133 treatment compared with the FFAs group (Fig. 5E-F). These results demonstrate that both CB1 and CB2 are capable of functionally regulating the Akt/GSK3β/Nrf2 pathway in hepatocytes, with CB1 acting as a negative regulator and CB2 as a positive regulator.

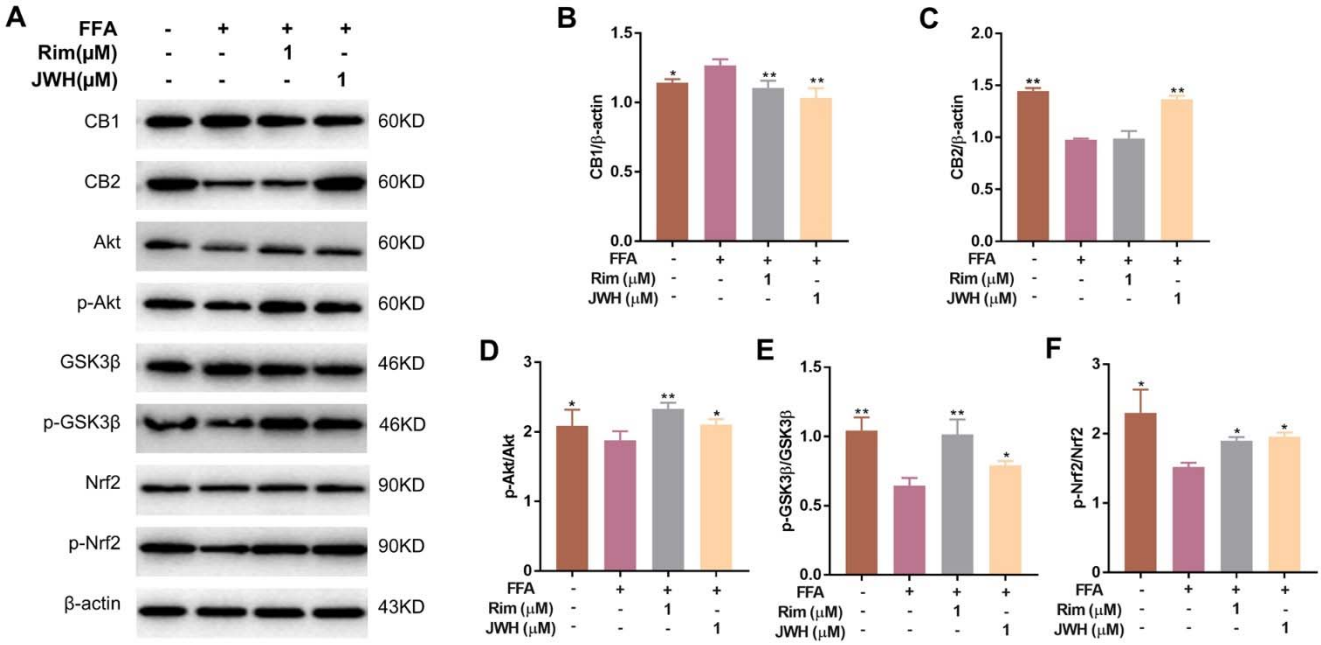

Fig. 5. Effects of the CB1 antagonist Rimonabant or the CB2 agonist JWH-133 on Akt signaling in FFAs-stimulated HepG2 cells. (A) Representative protein expression bands. (B-F) The quantification analysis for CB1, CB2, Akt, GSK3β and Nrf2. *$P < 0.05$, **$P < 0.01$, compared with the FFA group.

3.6 ZBA activates the Akt/GSK3β/Nrf2 pathway via dual modulation of CB1 and CB2

To investigate whether ZBA exerts its protective effects against MASLD through modulation of the CB1/CB2-Akt/GSK3β/Nrf2 axis, we examined the expression of endogenous cannabinoid receptors and downstream signaling proteins in FFAs-stimulated HepG2 cells and HFD-fed mice. Compared with the FFA group, low-dose ZBA slightly decreased CB1 expression and increased CB2 expression, whereas high-dose ZBA induced more pronounced changes (Fig. 6A-C). Correspondingly, phosphorylation levels of Akt,

GSK3β, and Nrf2 were significantly enhanced in the high-dose group (Fig. 6D-F), indicating activation of the CB1/CB2-Akt/GSK3β/Nrf2 pathway. Consistently, ELISA analysis revealed that ZBA reduced the elevated secretion of TNF-α, IL-1β, and IL-6, with high-dose treatment achieving the most pronounced anti-inflammatory effect (Fig. 6G-I). In HFD-fed mice, hepatic CB1 expression was markedly increased while CB2 expression was decreased compared with the normal group. Low-dose ZBA partially corrected CB1/CB2 levels, whereas high-dose ZBA significantly restored receptor expression (Fig. 7A-C). Similarly, phosphorylation of Akt, GSK3β, and Nrf2 was moderately increased in the low-dose group and significantly elevated in the high-dose group (Fig. 7D-F). Immunohistochemical staining further confirmed that ZBA decreased hepatic TNF-α, IL-1β, and IL-6 expression, with the significant effect observed at the high dose (Fig. 7G). Collectively, these findings demonstrate that ZBA ameliorates hepatic lipid accumulation and inflammatory responses through activation of the CB1/CB2-midiated Akt/GSK3β/Nrf2 signaling axis in both *in vitro* and *in vivo* MASLD models. Notably, a dose-responsive regulatory trend was observed, with pathway activation and anti-inflammatory effects becoming more pronounced at the higher dose.

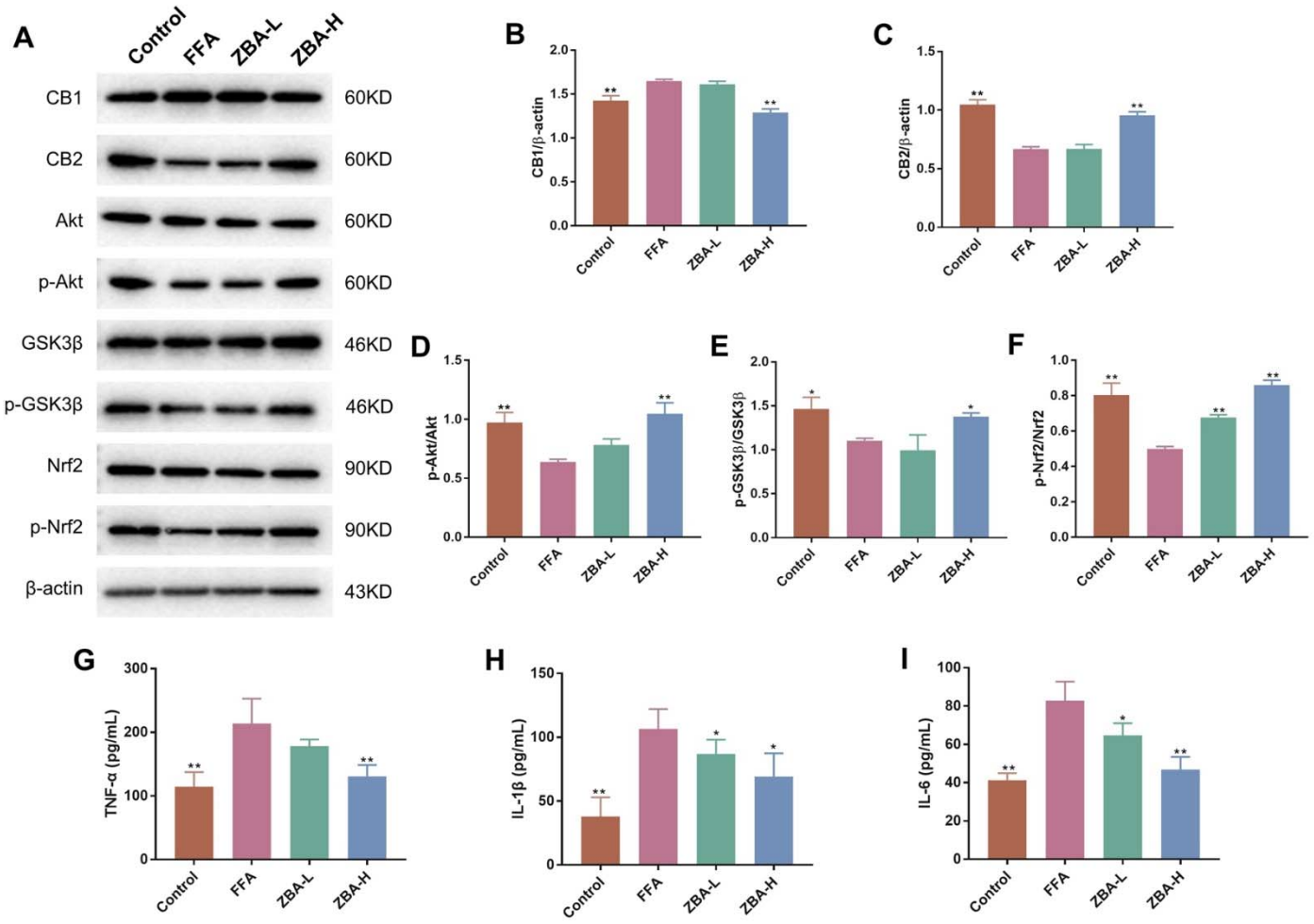

Fig. 6 Effect of ZBA on endogenous cannabinoid receptors and Akt/GSK3β/Nrf2 pathway in FFAs-stimulated HepG2 cells. (A) Representative protein expression bands. (B-F) The quantification analysis for CB1, CB2, Akt, GSK3β and Nrf2. (G-I) ELISA analysis of inflammatory factors. *$P < 0.05$, **$P < 0.01$, compared with the FFA group.

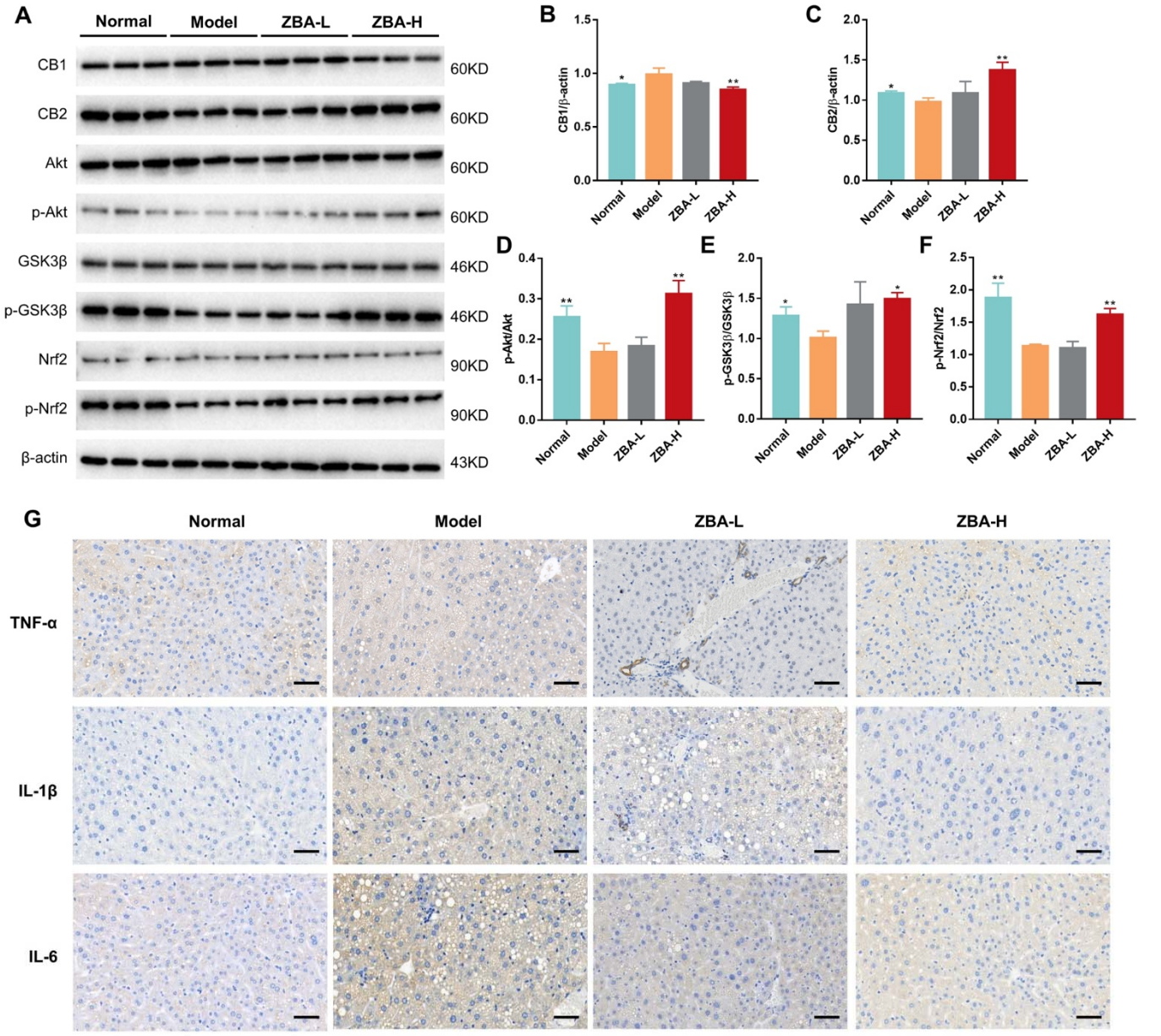

Fig. 7 Effect of ZBA on endogenous cannabinoid receptors and Akt/GSK3β/Nrf2 pathway in HFD-fed mice. (A) Representative protein expression bands. (B-F) The quantitative analysis of CB1, CB2, Akt, GSK3β and Nrf2 in the liver tissues. (G) Immunohistochemical staining for hepatic inflammatory factors in HFD-fed mice (200×, bar = 50 μm). *P < 0.05, **P < 0.01, compared with the model group.

4. Discussion

Huajiao is a spice with a long history and holds an important position in the culinary culture of China and East Asia. Beyond its role as a seasoning, it is widely recognized as an edible medicinal plant. Traditionally used to dispel dampness and manage colds and dysentery, modern research expanded have also revealed that *Huajiao* exhibits lipid-lowering and hepatoprotective effects [21, 22]. Alkaloids are the main active ingredients in the peel of *huajiao*, which may be candidate drugs for treating MASLD [18]. This study employed a laboratory optimization scheme to prepare standardized ZBA samples for subsequent pharmacological and mechanistic research [27].

In the established *in vitro* MASLD model of FFA-loaded HepG2 cells, ZBA effectively alleviated lipid accumulation, which was confirmed by a significant reduction in lipid droplets in Oil red O staining and a

decrease in intracellular TC and TG content. In the *in vivo* HFD-induced mice model, 12 weeks of ZBA treatment significantly ameliorated metabolic dysregulation and hepatic steatosis, as indicated by histopathological examination and biochemical assays. Furthermore, GTT and ITT results demonstrated that ZBA dose-dependently improved glucose tolerance and insulin sensitivity in HFD-fed mice. These results suggest that alkaloid-rich *huajiao* extract exerts beneficial effects against MASLD, supporting previous research findings [31].

There were diverse chemical components in ZBA, and 22 characteristic alkaloids were identified by UPLC-Q-TOF-MS/MS technology. These components provide the basis for ZBA to relieve MASLD. Consequently, we analyzed the potential action targets and synergistic networks of these components using network pharmacology and transcriptomics, which aligns well with the multi-components and holistic treatment in traditional Chinese medicine [32, 33]. Enrichment analysis revealed that ZBA treatment significantly affected pathways central to metabolism and inflammation, including insulin signaling, lipid and atherosclerosis, and TNF signaling. Key targets such as Akt, MTOR, TLR4, GSK3β, and CB1 were identified from this integrated analysis, highlighting their pivotal role in mediating the anti-MASLD effects of ZBA. Furthermore, molecular docking was employed to identify potential core targets. The results indicated that alkaloid components with high content in ZBA, such as hydroxy-α-sanshool and hydroxy-β-sanshool [27], exist a high affinity with three prominent target proteins—CB1, Akt, and GSK3β, among which the binding stability of CB1 with these components was higher, highlighting the central position of CB1 in the treatment of MASLD with ZBA.

The endocannabinoid system, particularly its classical receptors CB1 and CB2, has been increasingly recognized as a crucial regulator in MASLD pathophysiology [34, 35]. In the diseased liver, CB1 is pathologically upregulated and promotes *de novo* lipogenesis, insulin resistance, and mitochondrial dysfunction, whereas CB2 predominantly resides in Kupffer cells and hepatic stellate cells, where its activation exerts anti-inflammatory and anti-fibrotic effects [36-39]. Furthermore, the Akt/GSK3β/Nrf2 signaling axis is known to govern insulin sensitivity, lipid metabolism, and oxidative stress responses. Specifically, Akt phosphorylates and inactivates GSK3β, thereby enhancing glycogen synthesis and alleviating insulin resistance, and Nrf2 activation counteracts inflammation and oxidative damage [40, 41]. Although omics and network pharmacology data suggest that ZBA may regulate CB1, Akt, and GSK3β, it was unclear whether they acted in parallel or in a linear cascade. To address this question, we performed pharmacological intervention experiments using the selective CB1 antagonist Rimonabant and the selective CB2 agonist JWH-133 in FFAs-stimulated HepG2 cells. The results demonstrate that blocking CB1 or activating CB2 directly dictates the phosphorylation state of Akt, which subsequently governs the p-GSK3β/p-Nrf2 cascade. Mechanistically, pathological overstimulation of peripheral CB1 impairs insulin receptor substrate-1 signaling, placing an upstream molecular brake on PI3K/Akt recruitment [14]. By dismantling this brake through CB1 antagonism, Akt is activated by phosphorylation, which leads to the

inhibitory phosphorylation of GSK3β and activating phosphorylation. These findings provide the direct evidence that CB1 and CB2 function as upstream regulators of the Akt/GSK3β/Nrf2 signaling axis.

ZBA treatment further clarified the therapeutic relevance of the CB1/CB2-midiated Akt/GSK3β/Nrf2 axis. The high-dose ZBA exhibited a significant dual modulatory effect on CB1/CB2, thereby activating the Akt/GSK3β/Nrf2 pathway, while low-dose treatment also induced a consistent regulatory trend across multiple molecular and phenotypic indicators. However, the magnitude of the dose response appeared to differ between upstream signaling molecules and downstream biological outcomes. Restoration of CB1/CB2 expression and phosphorylation of Akt, Nrf2 and GSK3β were more evident at the higher dose, whereas improvements in downstream phenotypic markers and suppression of pro-inflammatory cytokines in some cases significant, following low-dose intervention. Such observations may be related to the hierarchical nature of receptor-mediated signal transduction. In signaling cascades, relatively modest alterations at the receptor or kinase level can be progressively amplified through downstream signaling events, thereby enabling measurable biological responses when upstream changes remain limited [42]. This phenomenon may explain why clear improvements in inflammatory status, lipid accumulation, and metabolic parameters were observed despite comparatively moderate modulation of upstream molecular targets under low-dose treatment conditions. Therefore, the therapeutic effects of ZBA may not limited to a single activation threshold but rather reflect a progressive regulation of the CB1/CB2-Akt/GSK3β/Nrf2 signaling network. Therefore, ZBA exhibits a dose-responsive regulatory trend in the mitigation of MASLD.

The activation of the Akt/GSK3β/Nrf2 pathway by ZBA leads to a systemic alleviation of MASLD symptoms, which is related to the modulation of glucose metabolism and the hepatic inflammatory microenvironment. Metabolic insulin resistance and chronic low-grade inflammation are crucial in MASLD progression, wherein impaired insulin signaling fosters systemic glucose intolerance and increases lipogenic substrate [43]. ZBA dose-dependently improved glucose tolerance and insulin sensitivity. This functional rescue is strongly aligned with the restoration of the Akt/GSK3β cascade. Activation of Akt and the subsequent inhibitory phosphorylation of GSK3β alleviate insulin resistance, and reduces the systemic metabolic cross-talk [44]. Moreover, the upregulation of CB2 and the subsequent increase in Nrf2 phosphorylation led to a marked reduction in pro-inflammatory cytokines, effectively neutralizing lipotoxic stress and preventing inflammatory cell infiltration in liver tissue [45]. These results indicate that ZBA has the characteristic of multi-target intervention in MASLD.

Given the rising global prevalence of MASLD and a lack of therapeutic drugs, there is an expanding market demand for safe and natural interventions [4]. ZBA, derived from the widely consumed medicinal and edible spice *Z. bungeanum*, possesses unique multi-target advantages and high safety profiles. Its clinical and commercial translation could thus effectively meet the healthcare needs for metabolic liver diseases. However, several critical considerations should be addressed to realize this potential. Preclinical pharmacokinetic evidence indicates that the major bioactive alkylamides in ZBA, such as hydroxy-α-sanshool, are rapidly absorbed upon oral ingestion, yet they undergo significant metabolism,

resulting in moderate oral bioavailability and relatively rapid clearance [46, 47]. Structurally, the alkylamides in ZBA are polyunsaturated aliphatic amides that exhibit high structural homology and conformational mimicry with endogenous cannabinoids, granting them inherent gastrointestinal mucosa permeability [48]. Furthermore, our findings demonstrated that ZBA exhibits specific binding to both CB1 and CB2 receptors, suggesting that sufficient systemic exposure and hepatic accumulation are necessary to saturate and modulate these therapeutic targets. In addition to these pharmacokinetic traits, the polyunsaturated amides abundant in ZBA face practical hurdles, including poor chemical stability against oxidation and intense, pungent, and tongue-numbing sensory properties [18]. Therefore, the future development of ZBA-based functional foods or therapeutic agents requires the adoption of advanced food or pharmaceutical engineering strategies, such as microencapsulation technologies or lipid-based nanoemulsions. These approaches could critically enhance the structural stability, target-specific absorption, and palatability of ZBA, thereby promoting the care of MASLD.

5. Conclusion

The present study demonstrates that ZBA exerts potent protective effects against MASLD by functioning as a dual modulator of the endocannabinoid system, inhibiting CB1 and activating CB2. CB1 and CB2 serve as upstream regulators of the Akt/GSK3β/Nrf2 signaling axis, and activation of this cascade by ZBA reduces hepatic lipid accumulation, improves insulin sensitivity, and suppresses inflammatory responses. These consistent effects in cell and animal models highlight the potential of ZBA derived from *huajiao* as a dietary active ingredient for MASLD, providing a basis for its development as a natural dietary supplement or intervention strategy.

Conflict of interest

All authors declare that no conflict of interest exists.

Acknowledgments

This work was supported by the National Natural Science Foundation of China (82304813), and the Three Sailing Talents Cultivation Program of Naval Medical University. We thank the platform provided by BioGDP.com for drawing graphic abstract.

References

[1] Corrao S, Calvo L, Grana W, et al., Metabolic dysfunction-associated steatotic liver disease: A pathophysiology and clinical framework to face the present and the future, Nutr. Metab. Cardiovasc. Dis. 35 (2025) 103702. https://doi.org/10.1016/j.numecd.2024.07.019.

[2] Huang DQ, Wong VWS, Rinella ME, et al., Metabolic dysfunction-associated steatotic liver disease in adults, Nat. Rev. Dis. Primers. 11 (2025) 14. https://doi.org/10.1038/s41572-025-00599-1.

[3] Zeng J, Fan JG, Francque SM, Therapeutic management of metabolic dysfunction associated steatotic liver disease, United Eur. Gastroent. 12 (2024) 177-186. https://doi.org/10.1002/ueg2.12525.

[4] Younossi ZM, Zelber-Sagi S, Henry L, et al., Lifestyle interventions in nonalcoholic fatty liver disease, Nat. Rev. Gastroenterol. Hepatol. 20 (2023) 708-722. https://doi.org/10.1038/s41575-023-00800-4.

[5] Chang Z, Xu X, Xu Y, et al., Potential Effects of Functional Foods and Dietary Supplements on Metabolic-Associated Fatty Liver Disease and the Underlying Mechanisms: A Narrative Review with a Focus on the Modulation of the Gut Microbiota, J. Agric. Food Chem. 73 (2025) 29247-29280. https://doi.org/10.1021/acs.jafc.5c05587.

[6] Zeng Y, Wu R, Wang F, et al., Liberation of daidzein by gut microbial beta-galactosidase suppresses acetaminophen-induced hepatotoxicity in mice, Cell Host Microbe. 31 (2023) 766-780. https://doi.org/10.1016/j.chom.2023.04.002.

[7] Song W, Hu JH, Zhu LN, et al., Inulin alleviates HFD-induced NAFLD by hepatic macrophage polarization and lipid metabolism via gut-liver axis, Food Sci. Hum. Wellness 14 (2025). https://doi.org/Artn 925004010.26599/Fshw.2024.9250040.

[8] Liu W, Sun M, Zhang H, et al., Targeting regulation of lipid metabolism with polysaccharide of traditional Chinese medicine for the treatment of non-alcoholic fatty liver disease: A review, Int. J. Biol. Macromol. 306 (2025) 141660. https://doi.org/10.1016/j.ijbiomac.2025.141660.

[9] Liang W, Zhou K, Jian P, et al., Ginsenosides Improve Nonalcoholic Fatty Liver Disease via Integrated Regulation of Gut Microbiota, Inflammation and Energy Homeostasis, Front. Pharmacol. 12 (2021) 622841. https://doi.org/10.3389/fphar.2021.622841.

[10] Wang K, Jia W, Huang Z, et al., Research progress of the protection provided by traditional Chinese medicine on non-alcoholic fatty liver disease via regulating liver macrophages, Acta Pharmacol. Sin. 59 (2024) 801-810. https://doi.org/10.16438/j.0513-4870.2023-1100.

[11] Bazwinsky-Wutschke I, Zipprich A, Dehghani F, Endocannabinoid System in Hepatic Glucose Metabolism, Fatty Liver Disease, and Cirrhosis, Int. J. Mol. Sci. 20 (2019) 2516. https://doi.org/10.3390/ijms20102516.

[12] Mboumba Bouassa RS, Sebastiani G, Di Marzo V, et al., Cannabinoids and Chronic Liver Diseases, Int. J. Mol. Sci. 23 (2022) 9423. https://doi.org/10.3390/ijms23169423.

[13] Rossi F, Punzo F, Umano GR, et al., Role of Cannabinoids in Obesity, Int. J. Mol. Sci. 19 (2018) 2690. https://doi.org/10.3390/ijms19092690.

[14] Liu J, Zhou L, Xiong K, et al., Hepatic cannabinoid receptor-1 mediates diet-induced insulin resistance via inhibition of insulin signaling and clearance in mice, Gastroenterology 142 (2012) 1218-1228. https://doi.org/10.1053/j.gastro.2012.01.032.

[15] Turcotte C, Blanchet MR, Laviolette M, et al., The CB2 receptor and its role as a regulator of inflammation, Cell Mol. Life Sci. 73 (2016) 4449-4470. https://doi.org/10.1007/s00018-016-2300-4.

[16] Louvet A, Teixeira-Clerc F, Chobert MN, et al., Cannabinoid CB2 receptors protect against alcoholic liver disease by regulating Kupffer cell polarization in mice, Hepatology 54 (2011) 1217-1226. https://doi.org/10.1002/hep.24524.

[17] Ghasemi-Gojani E, Kovalchuk I, Kovalchuk O, Cannabinoids and terpenes for diabetes mellitus and its complications: from mechanisms to new therapies, Trends Endocrinol. Metab. 33 (2022) 828-849. https://doi.org/10.1016/j.tem.2022.08.003.

[18] Liang W, Yang H, Lei H, et al., Phytochemistry and health functions of Zanthoxylum bungeanum Maxim and Zanthoxylum schinifolium Sieb. et Zucc as pharma-foods: A systematic review, Trends Food Sci. Tech. 143 (2024) 104225. https://doi.org/10.1016/j.tifs.2023.104225.

[19] Shaoyang X, Yanxiu G, Xiaohui M, et al., Research progress on chemical constituents and pharmacological effects of Zanthoxylum, West China J. Pharm. Sci. 36 (2021) 717-722. https://doi.org/10.13375/j.cnki.wcjps.2021.06.027.

[20] Shi W-J, Chai T, Lv C-M, et al., Research progress on the main flavor components and detection methods of Zanthoxylum bungeanum Maxim., J. Food Compos. Anal. 144 (2025) 107658. https://doi.org/10.1016/j.jfca.2025.107658.

[21] Guo J, He C-X, Zhang Q, et al., The pericarp of Zanthoxylum bungeanum Maxim.: An excellent source for the development of alternative drugs for improving glucose and lipid metabolism disorder related diseases, Arab. J. Chem. 17 (2024) 105594. https://doi.org/ 10.1016/j.arabjc.2023.105594.

[22] Huang X, Yuan Z, Liu X, et al., Integrative multi-omics unravels the amelioration effects of Zanthoxylum bungeanum Maxim. on non-alcoholic fatty liver disease, Phytomedicine 109 (2023) 154576. https://doi.org/10.1016/j.phymed.2022.154576.

[23] Gu G, Yang Y, Zhang F, et al., Critical review on biological effects and mechanisms of amide alkaloids in Piper nigrum and Piper longum, Food Med. Homology. 3 (2026) 9420083. https://doi.org/https://doi.org/10.26599/fmh.2026.9420083.

[24] You Y, Ren T, Zhang S, et al., Hypoglycemic effects of Zanthoxylum alkylamides by enhancing glucose metabolism and ameliorating pancreatic dysfunction in streptozotocin-induced diabetic rats, Food Funct. 6 (2015) 3144-3154. https://doi.org/10.1039/c5fo00432b.

[25] Ren T, Zhu Y, Xu F, et al., The mechanisms of hydroxy-α-sanshool from Zanthoxyum bungeanum maxim activates AMPK-HIF1-PKM2 pathway to fix the obesity, J. Funct. Foods 107 (2023) 105599. https://doi.org/ 10.1016/j.jff.2023.105599.

[26] Zhang Q, He CX, Wang LY, et al., Hydroxy-alpha-sanshool from the fruits of Zanthoxylum bungeanum Maxim. promotes browning of white fat by activating TRPV1 to induce PPAR-gamma deacetylation, Phytomedicine. 121 (2023) 155113. https://doi.org/10.1016/j.phymed.2023.155113.

[27] Heying Y, Caiping L, Ting P, et al., Optimization of purification process and component analysis of alkaloids from Zanthoxylum bungeanum Maxim, J. Pharm. Practice Service 43 (2025) 75-81.

[28] Hirsch S, Hinden L, Naim MB, et al., Hepatic targeting of the centrally active cannabinoid 1 receptor (CB_1R) blocker rimonabant via PLGA nanoparticles for treating fatty liver disease and diabetes, J. Controlled Release 353 (2023) 254-269. https://doi.org/10.1016/j.jconrel.2022.11.040.

[29] De Gottardi A, Spahr L, Ravier-Dall'Antonia F, et al., Cannabinoid receptor 1 and 2 agonists increase lipid accumulation in hepatocytes, Liver Int. 30 (2010) 1482-1489. https://doi.org/10.1111/j.1478-3231.2010.02298.x.

[30] Scandiffio R, Bonzano S, Cottone E, et al., Beta-Caryophyllene Modifies Intracellular Lipid Composition in a Cell Model of Hepatic Steatosis by Acting through CB2 and PPAR Receptors, Int. J. Mol. Sci. 24 (2023) 6060. https://doi.org/10.3390/ijms24076060.

[31] Peng W, He CX, Li RL, et al., Zanthoxylum bungeanum amides ameliorates nonalcoholic fatty liver via regulating gut microbiota and activating AMPK/Nrf2 signaling, J. Ethnopharmacol. 318 (2024) 116848. https://doi.org/10.1016/j.jep.2023.116848.

[32] Zhu X, Yao Q, Yang P, et al., Multi-omics approaches for in-depth understanding of therapeutic mechanism for Traditional Chinese Medicine, Front. Pharmacol. 13 (2022) 1031051. https://doi.org/10.3389/fphar.2022.1031051.

[33] Li S, Zhang B, Traditional Chinese medicine network pharmacology: theory, methodology and application, Chin. J. Nat. Med. 11 (2013) 110-120. https://doi.org/10.1016/S1875-5364(13)60037-0.

[34] Cani PD, Plovier H, Van Hul M, et al., Endocannabinoids - at the crossroads between the gut microbiota and host metabolism, Nat. Rev. Endocrinol. 12 (2016) 133-143. https://doi.org/10.1038/nrendo.2015.211.

[35] Maccarrone M, Di Marzo V, Gertsch J, et al., Goods and Bads of the Endocannabinoid System as a Therapeutic Target: Lessons Learned after 30 Years, Pharmacol. Rev. 75 (2023) 885-958. https://doi.org/10.1124/pharmrev.122.000600.

[36] De Gottardi A, Spahr L, Ravier-Dall'Antonia F, et al., Cannabinoid receptor 1 and 2 agonists increase lipid accumulation in hepatocytes, Liver Int. 30 (2010) 1482-1489. https://doi.org/10.1111/j.1478-3231.2010.02298.x.

[37] Irungbam K, Churin Y, Matono T, et al., Cannabinoid receptor 1 knockout alleviates hepatic steatosis by downregulating perilipin 2, Lab. Invest. 100 (2020) 454-465. https://doi.org/10.1038/s41374-019-0327-5.

[38] Tedesco L, Valerio A, Dossena M, et al., Cannabinoid receptor stimulation impairs mitochondrial biogenesis in mouse white adipose tissue, muscle, and liver: the role of eNOS, p38 MAPK, and AMPK pathways, Diabetes 59 (2010) 2826-2836. https://doi.org/10.2337/db09-1881.

[39] Hirsch S, Hinden L, Naim MB, et al., Hepatic targeting of the centrally active cannabinoid 1 receptor (CB(1)R) blocker rimonabant via PLGA nanoparticles for treating fatty liver disease and diabetes, J Control Release. 353 (2023) 254-269. https://doi.org/10.1016/j.jconrel.2022.11.040.

[40] Xiaofei Z, Xiaolei G, Xiaotong L, et al., The role of GSK3β in adipose tissue inflammation induced by bisphenol-A in high fat diet fed mice, J. Hygiene Research 48 (2019) 964-969. https://doi.org/10.19813/j.cnki.weishengyanjiu.2019.06.017.

[41] Dodson M, de la Vega MR, Cholanians AB, et al., Modulating NRF2 in Disease: Timing Is Everything, Annu. Rev. Pharmacol. Toxicol. 59 (2019) 555-575. https://doi.org/10.1146/annurev-pharmtox-010818-021856.

[42] Hunter T, Signaling—2000 and Beyond, Cell 100 (2000) 113-127. https://doi.org/10.1016/s0092-8674(00)81688-8.

[43] Byrne CD, Armandi A, Pellegrinelli V, et al., Muetabolic dysfunction-associated steatotic liver disease: a condition of heterogeneous metabolic risk factors, mechanisms and comorbidities requiring holistic treatment, Nat. Rev. Gastroenterol. Hepatol. 22 (2025) 314-328. https://doi.org/10.1038/s41575-025-01045-z.

[44] Bo T, Gao L, Yao Z, et al., Hepatic selective insulin resistance at the intersection of insulin signaling and metabolic dysfunction-associated steatotic liver disease, Cell Metab. 36 (2024) 947-968. https://doi.org/10.1016/j.cmet.2024.04.006.

[45] Wu Q, Ma Y, Liu Y, et al., CB2R agonist JWH-133 attenuates chronic inflammation by restraining M1 macrophage polarization via Nrf2/HO-1 pathway in diet-induced obese mice, Life Sci. 260 (2020) 118424. https://doi.org/10.1016/j.lfs.2020.118424.

[46] Rong R, Cui MY, Zhang QL, et al., Anesthetic constituents of Zanthoxylum bungeanum Maxim.: A pharmacokinetic study, J. Sep. Sci. 39 (2016) 2728-2735. https://doi.org/10.1002/jssc.201600295.

[47] Meng J, Qian D, Li RL, et al., In Vitro Metabolism and In Vivo Pharmacokinetics Profiles of Hydroxy-alpha-Sanshool, Toxics 12 (2024) 100. https://doi.org/10.3390/toxics12020100.

[48] Dossou KS, Devkota KP, Morton C, et al., Identification of CB1/CB2 ligands from Zanthoxylum bungeanum, J. Nat. Prod. 76 (2013) 2060-2064. https://doi.org/10.1021/np400478c.